VIII International Conference on Computational Methods for Coupled Problems in Science and Engineering
COUPLED PROBLEMS 2019
E. Oñate, M. Papadrakakis and B. Schrefler (Eds)

COUPLED PORO-INELASTIC RESPONSE OF SOILS USING A NEW INTERPOLATION RULE THROUGH THE GENERALIZED PLASTICITY THEORY WITHIN THE UBCSAND MODEL

E. TATLIOGLU[†], M.B.C. ULKER*

[†] Earthquake Engineering and Disaster Management Institute (EEDMI)
Istanbul Technical University
Ayazaga Campus, 34469 Istanbul, Turkey
Email: esrakahraman@itu.edu.tr

* Earthquake Engineering and Disaster Management Institute (EEDMI)
Istanbul Technical University
Ayazaga Campus, 34469 Istanbul, Turkey
Email: mbulker@itu.edu.tr – web page: http://www.eedmi.itu.edu.tr

Key words: Cyclic behavior, Generalized plasticity, Interpolation rule, Sandy soils, Poroelasticity.

Abstract. During numerical computations, when the stress is updated in the constitutive relationship, it is of major necessity to distinguish the soil behavior under cyclic or transient loads from that of monotonic ones. The cyclic plasticity models developed to simulate the mechanism of soil failure, require accurate predictions of irreversible strains computed through a flow rule in both virgin loading and stress reversals. In multi-surface type models, such as UBCSAND, plastic modulus is calculated using a hardening rule where the location of the current stress tensor is related to its projection on the bounding surface through an interpolation rule.

In this study, the plastic hardening modulus (H_L) that is calculated using the Generalized Plasticity Theory, is adapted in the current formulation of the UBCSAND hardening rule in terms of deviatoric plastic strains. Hence, the UBCSAND model is modified to serve with the generalized plasticity framework to evaluate the cyclic behavior of sands. This way of calculating the plastic modulus is based upon an interpolation rule that typically exists in the bounding surface theory with the value of H_L on the bounding surface. Such a concept is very well applicable to clay soils also.

Firstly, a number of strain and stress-controlled cyclic triaxial tests are simulated in order to validate the current constitutive formulation. Secondly, the effects of the new interpolation rule on the cyclic behavior of granular soils is investigated with a number of parametric studies which are performed to examine the effect of H_L on the overall cyclic response. Finally, the new formulation is implemented in an in-house finite element code developed to solve the coupled equations of the partially dynamic (PD) Biot formulation used to analyse a soil-column problem under harmonic surface excitation. Results are obtained in terms of solid displacement, pore pressure and effective stress variation in temporal and spatial domains.

1 INTRODUCTION

Elasto-plastic response of soils are evaluated based upon the valid assumption that the constitutive behavior of soils is inherently nonlinear under applied loads beyond a certain strain level. Such a phenomenon becomes particularly important when the coupled flow and deformation response of soils is taken into consideration in solution of related geomechanics problems, hence the theory of poro-inelasticity. Therefore, one should adopt a coupled mathematical formulation, such as that of Biot's theory for porous media, and make use of a nonlinear elasto-plastic model governing essentially the effective stress-strain relationship. While such a process is applicable to all soils and geomechanics problems, this is by no means a trivial process. That is, finding a constitutive model that is capable of capturing the most essential features of soil dynamic behavior under cyclic loading caused by earthquakes or ocean waves and yet keeping the theory as simple as possible is the most challenging task of all. In this study, such an objective is set with the idea of enhancing a well-known constitutive model, UBCSAND, which is used to model the cyclic response of loose sands through the basic notions of another simple theory called the Generalized Plasticity Theory (GPT). A simple hardening interpolation rule is proposed to calculate the plastic hardening modulus with an analogy to bounding surface plasticity concept.

GPT was proposed to encompass the existing theories in a unified manner acting as a more general theory which allows the inclusion of main features of other frameworks (Pastor et al., 1985; Pastor et al., 1990). This property of the GPT comes from the fact that it is a very flexible theory leading to a model that captures observed fundamental behavior under static and dynamic loading. It requires only the loading/unloading directions, a plastic flow direction, a plastic hardening modulus in loading/unloading, and an elasticity matrix. These main properties of the theory are adapted to work within UBCSAND to enhance its capability towards modeling undrained cyclic triaxial behavior of sands. A number of strain and stress-controlled undrained cyclic triaxial tests are simulated in order to validate the current constitutive formulation. Then the effects of the new interpolation rule on the liquefaction behavior of loose sands is investigated in a few parametric studies which are performed to examine the effect of hardening modulus on liquefaction. Finally, the new formulation is implemented in a new finite element code developed to solve the coupled equations of the partially dynamic (PD) Biot formulation used to analyse a soil-column problem under harmonic surface excitation.

2 UBCSAND MODEL

The formulation of the original UBCSAND model is based on classical plasticity theory. In order to model the behavior of sandy soils in static and dynamic conditions, UBCSAND model was first developed by Puebla et al. (1997) and later Beaty and Byrne (1998) at the University of British Columbia (UBC). In this initial version of the model, mathematical formulation is implemented to work for the plane stress state. Then Tsegaye (2010) extended the model to work for three-dimensional (3-D) problems which was termed the UBC-PLM model. Also, Petalas and Galavi (2012) and Petalas et al. (2013) made some improvements to the model to better explain the soil behavior under dynamic loading. Below summarizes the fundamentals.

2.1 Mathematical formulation

Elastic behavior

The elastic behavior within the yield surface is governed by a non-linear rule as a function of mean effective stress. Two parameters that control the nonlinear elastic behavior are the elastic bulk modulus, K and shear modulus, G calculated using the following relations:

$$K = k_B^e.P_A.(\frac{p'}{P_A})^{me} \tag{1}$$

$$G = k_G^e.P_A.(\frac{p'}{P_A})^{ne} \tag{2}$$

where k_B^e and k_G^e are the elastic bulk and shear moduli at the reference stress level, P_A which is the atmospheric pressure, p' is the effective stress, me and ne are the model parameters.

Yield function

UBCSAND model uses the well-known Mohr-Coulomb yield function generalized in 3-D principal stress space given as:

$$f_m = \frac{\sigma'_{\max} - \sigma'_{\min}}{2} - \left(\frac{\sigma'_{\max} + \sigma'_{\min}}{2} + c' \cot \phi_p \right) \sin \phi_m \tag{3}$$

where $\sigma'_{\max}$ and $\sigma'_{\min}$ are the maximum and minimum effective stresses, c' is the effective cohesion of the soil, ϕ_p is the peak friction angle and ϕ_m is the mobilized friction angle during hardening. The yield surface defined in terms of the principal stresses can be written in terms of stress invariants, including shear stresses without departing from the actual theory:

$$f\left(\sigma, \sin \varphi_m\right) = \bar{\sigma} - M.I = 0 \tag{4}$$

where $\bar{\sigma} = \sqrt{3J_2}$, $I = I_1/3$ with I_1 being the first invariant of stress and J_2 is the second deviatoric stress invariant. M determines the position of the yield surface and depends on the third stress invariant, J_3, Lode's angle (θ) and the hardening parameter, $\sin \varphi_m$. Thus we have:

$$M = \frac{6 \sin \varphi_m}{3 - \sin \varphi_m \sin 3\theta} \tag{5}$$

and the θ:

$$\theta = \frac{1}{3} \sin^{-1} \left(-\frac{3\sqrt{3}}{2} \frac{J_3}{J_2^{3/2}} \right), \quad -\frac{\pi}{6} \le \theta \le \frac{\pi}{6} \tag{6}$$

Elasto-plastic behavior

When the stress vector reaches the yield surface, plastic deformations begin to occur. In the model, a non-associated flow rule is considered for the calculation of the plastic deformations using the plastic potential function defined as:

$$g(\sigma) = \bar{\sigma} - M^* I = 0 \tag{7}$$

Here, *M** depends on the mobilized dilation angle, ψ_m calculated similar to (5) as:

$$M^* = \frac{6\sin\psi_m}{3 - \sin\psi_m \sin 3\theta} \tag{8}$$

with

$$\sin\psi = \sin\varphi_m - \sin\varphi_{cv} \tag{9}$$

where φ_{cv} is the critical friction angle. Flow rule is written in a classical fashion as:

$$d\varepsilon^p = d\lambda \frac{\partial g}{\partial \sigma} \tag{10}$$

where $d\lambda$ is the plastic multiplier which defines plastic deformation amount and $\frac{\partial g}{\partial \sigma}$ describes the direction of the plastic deformation vector. Hardening law is defined by the hyperbolic relationship between the plastic shear strain and the mobilized friction angle which acts as the hardening parameter as per Puebla et al. (1997):

$$dsin\phi_m = G^* d\lambda dev\left(\frac{\partial g}{\partial \sigma}\right) \tag{11}$$

where G^* is the plastic shear modulus given as:

$$G^* = k_G^p \left(\frac{I}{P_A}\right)^{np-1} \left(1 - \frac{sin\phi_m}{sin\phi_p} * R_f\right)^2 \tag{12}$$

Here k_G^p is the plastic shear modulus number, *np* is the model parameter, P_A is the atmospheric pressure and $R_f = \frac{n_f}{n_{ult}}$ is the failure ratio generally ranging from 0.5 to 1.0 with n_f being the stress ratio at failure and n_{ult}, the ultimate stress ratio (Petalas et al., 2012).

Stress-strain relationship

The strain decomposition in an incremental form is written as,

$$d\underset{\sim}{\varepsilon} = d\underset{\sim}{\varepsilon}^e + d\underset{\sim}{\varepsilon}^p \tag{13}$$

where $d\varepsilon^e$ and $d\varepsilon^p$ are the elastic and plastic strain increments, respectively. Taking the elastic strains from this relation and using in the stress-strain relationship, we get:

$$d\underset{\sim}{\sigma} = \underset{\sim}{\underset{\sim}{D}}^{e}(d\underset{\sim}{\varepsilon} - d\underset{\sim}{\varepsilon}^{p}) \tag{14}$$

where D^e is the elastic constitutive matrix. Using the consistency condition with the inclusion of the hardening term gives:

$$\left(\frac{\partial f}{\partial \sigma}\right)^{T} D^{e}\left(d\varepsilon - d\lambda \frac{\partial g}{\partial \sigma}\right) + d\lambda \frac{\partial f}{\partial sin\phi_m}.G^{*}\sqrt{dev\frac{\partial g}{\partial \sigma}.dev\frac{\partial g}{\partial \sigma}}' = 0 \tag{15}$$

which is used to derive the final stress-strain relationship in incremental form as,

$$d\sigma = D^{e}\left(I - \frac{\frac{\partial g}{\partial \sigma}\left(\frac{\partial f}{\partial \sigma}\right)^{T} D^{e}}{\left(\frac{\partial f}{\partial \sigma}\right)^{T} D^{e}\frac{\partial g}{\partial \sigma} + H_L}\right) d\varepsilon \tag{16}$$

where the plastic modulus is:

$$H_L = -\frac{\partial f}{\partial sin\phi_m}.\frac{\partial sin\phi_m}{\partial \varepsilon_s^{p}}\sqrt{dev\frac{\partial g}{\partial \sigma}.dev\frac{\partial g}{\partial \sigma}}' \tag{17}$$

The tensor in (16) linking stress increments to strains is the 4th order elastoplastic matrix, D^{ep}.

Verification of the static behavior

Analyses are performed using a fully explicit forward Euler integration method for a representative soil element. Figure 1 shows the comparison of triaxial tests (Eliadorani, 2000) and the simulation results. Comparisons are made in terms of shear stress-axial strain relationships as well as stress path plots for fully undrained and partially drained tests. Partial drainage condition is defined as; $d\varepsilon_p = -d\varepsilon_1$ where $d\varepsilon_p$ is the total volumetric strain. Figure 2 presents the results for the fully drained condition obtained by Tatlıoğlu, (2018), which are compared with the tests of Tsegaye, (2010). Overall the presented formulation of the model is capable of capturing the main features of sand behavior under monotonic loading for three drainage conditions.

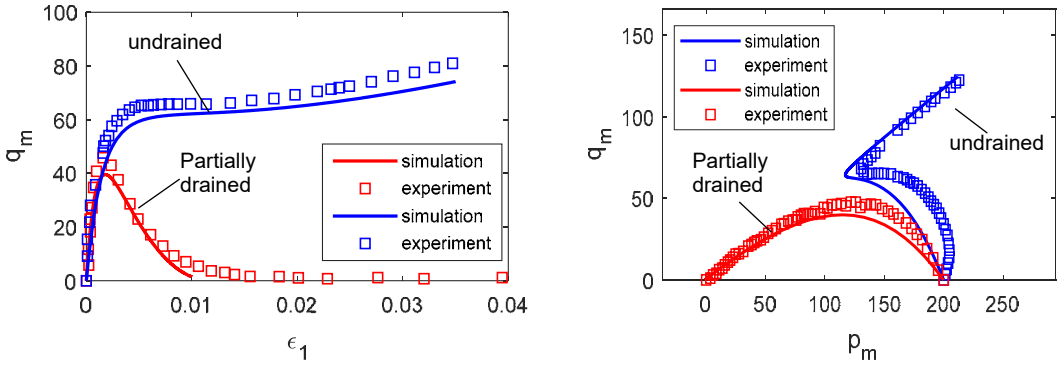

Figure 1: Simulation of undrained and partially drained triaxial test (Tatlıoğlu, 2018; data of Eliadorani, 2000)

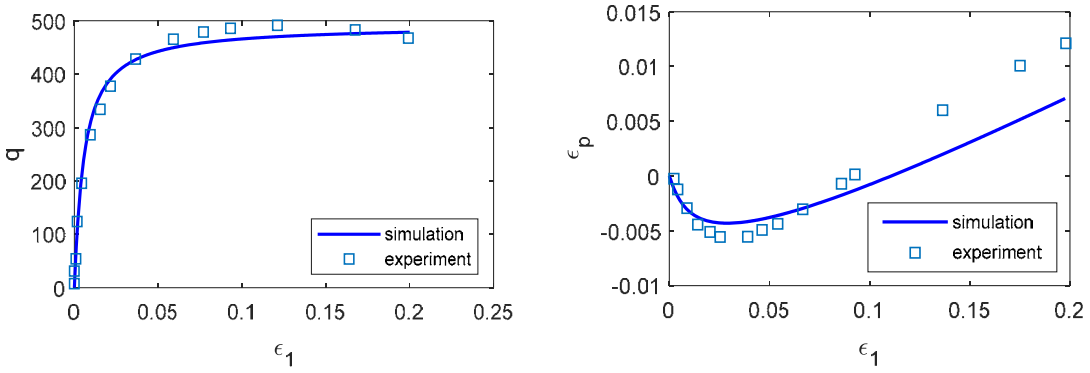

Figure 2: Simulation of drained triaxial test (Tatlıoğlu, 2018; data of Tsegaye, 2010)

2.2 Formulation for cyclic behavior using GPT

UBCSAND cyclic model

In the UBCSAND model, two different surfaces are defined: the primary and the secondary yield surface. The primary yield surface is active during the primary loading when it expands following the isotropic hardening rule until it reaches the maximum stress ratio. The secondary yield surface moves with a simplified kinematic hardening rule and is active after one loading-unloading step (Petalas et. al., 2012). The same yield surface definition is used for both surfaces. However, a different hardening rule is defined for each surface through the hardening parameter, $\sin\varphi_m$. The difference between the hardening rules used on these yield surfaces is due to the parameter, k_G^p used in G^* calculated as:

$$G^* = k_G^p \left(\frac{I}{P_A}\right)^{np-1} \left(1 - \frac{sin\phi_m}{sin\phi_p} * R_f\right)^2 \tag{18}$$

where k_G^p is taken constant during isotropic hardening. When the stress vector is on the secondary yield surface during stress reversals, k_G^p is a function of the number of cycles of loading;

$$k_G^p = k_G^p * \left(4 + \frac{n}{2}\right) * k_d * f_d \tag{19}$$

Here n is the number of stress reversals, k_d is the correction factor for loose soils calculated as below and f_d is a material parameter; $k_d = \min(1, \max(0.5, 0.1N_{1.60})$ (Petalas et. al., 2012).

Formulation of stress reversals using GPT

Generalized Plasticity Theory (GPT), capture the stress-strain relationship as observed in laboratory tests through minimum possible complexity. This means, the model is able to capture the actual behavior of soils by keeping the number of model parameters at a minimum (Ülker, 2016). Generalized Plasticity Model (GPM) is flexible enough to be used together with other models. In this study, it is aimed to improve the UBCSAND soil model with the

contribution of some of the features of GPM to better explain the dynamic behavior of sands.

In GPT, unit vector definition is used to decide loading and unloading steps in terms of *f*:

$$n = \frac{\partial f}{\partial \sigma} \Big/ \left| \frac{\partial f}{\partial \sigma} \right| \tag{20}$$

The direction of plastic flow is also calculated with unit vectors using the *g* surface through:

$$n_g = \frac{\partial g}{\partial \sigma} \Big/ \left| \frac{\partial g}{\partial \sigma} \right| \tag{21}$$

The following conditions are checked to decide the loading and unloading steps (Pastor et al., 1985; Pastor et al., 1990) in the case of hardening behavior:

$$d\sigma : n > 0 \rightarrow loading \ , \ d\sigma : n < 0 \rightarrow unloading \ , \ d\sigma : n = 0 \rightarrow neutral \ loading \tag{22}$$

Finally, the stress-strain relationship is obtained in the same way as in equation (16):

$$d\sigma = \left(D^e - \frac{D^e n_g n^T D^e}{H_L + n^T D^e n_g} \right) d\varepsilon \tag{23}$$

where the plastic hardening modulus is obtained with a reference to a consistency condition:

$$H_L = -\left[\frac{df}{d\sin\phi_m} \frac{d\sin\phi_m}{d\varepsilon^p} \right] \frac{dg}{d\sigma} \Big/ \left(\left| \frac{df}{d\sigma} \right| \left| \frac{dg}{d\sigma} \right| \right) \tag{24}$$

New interpolation rule for the plastic hardening modulus

In order to improve the simulation of dynamic behavior of sandy soils, plastic hardening modulus (H_L) that is calculated in its original form in the GPT, is now adapted in the current formulation of the hardening rule of UBCSAND using deviatoric plastic strains. When the stress vector lies on the secondary yield surface, the interpolation rule ensures the calculation of plastic modulus from primary loading. The following simple relation is proposed:

$$H_L^{\text{sec}} = H_L^{prim} \left(\frac{\sigma_U}{\sigma} \right)^{\gamma} \tag{25}$$

where H_L^{prim} is the value of the plastic modulus on the primary yield surface, σ is the current stress, σ_U is the stress value at the time of unloading and γ is the material parameter taken in this study as a function of accumulated plastic deviatoric strain, $\varepsilon_s^p = \int \left| d\varepsilon_s^p \right|$, defined as:

$$\gamma = \gamma_0 \exp\left(-D\varepsilon_s^p \right) \tag{26}$$

where $D>0$ is a proportionality constant and γ_0 is the initial value of γ.

2.3 Simulation of cyclic behavior

In this study, UBCSAND soil model with given interpolation rule of GPT is implemented in a

computer program which is verified with a number of cyclic undrained triaxial tests. Figure 3 shows a strain-controlled test simulation. Except for the primary loading, the actual cyclic trend leading to a decrease in the mean stress is well captured. This is also the case for plastic deviatoric strains used to update the hardening parameter. Figure 4 presents the stress-controlled triaxial test. Simulations are compared with the ones from Pastor et al. (1985). Hardening material parameters are taken as; D=300 and γ_0=20 for both simulations which seem to be the optimum values to obtain convergence for both of the analyses. As a result of these simulations, this simply modified UBCSAND model is in a better position to simulate undrained cyclic triaxial tests, particularly the liquefaction of loose sand which has been an issue for the original formulation of this model (Beaty and Byrne, 1998).

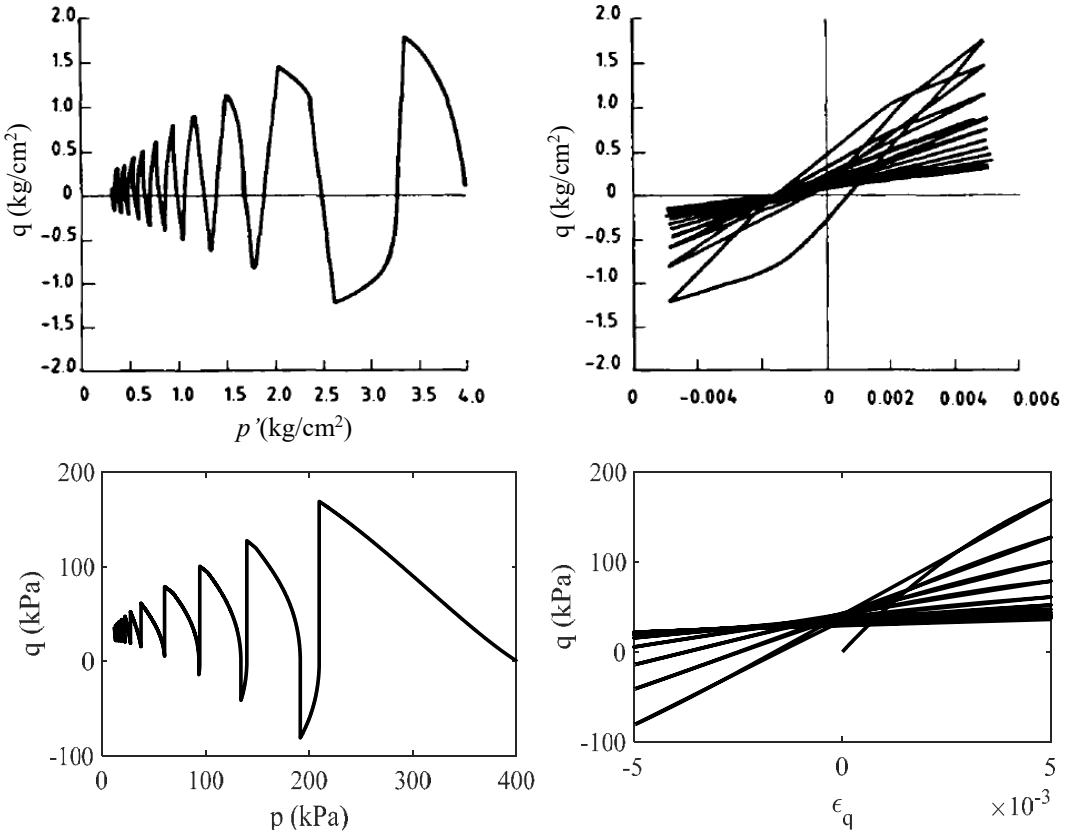

Figure 3: Simulation of strain-controlled undrained cyclic triaxial test as compared to Pastor et al. (1985)

3 IMPLEMENTATION INTO FINITE ELEMENT METHOD

3.1 PD formulation of Biot poroelasticity

The dynamic behavior of loose sands requires the solution of coupled flow and deformation equations proposed by Biot (1941, 1955, 1962). These equations are derived from the conservation of momentum and mass as well as the inclusion of a valid constitutive law for the stress-strain relationship of the solid skeleton of the soil. D'Arcy's law is also

added to govern the pore water flow. By ignoring the inertial forces associated with the pore water, the equations can be written in the Partially Dynamic (PD) form as follows:

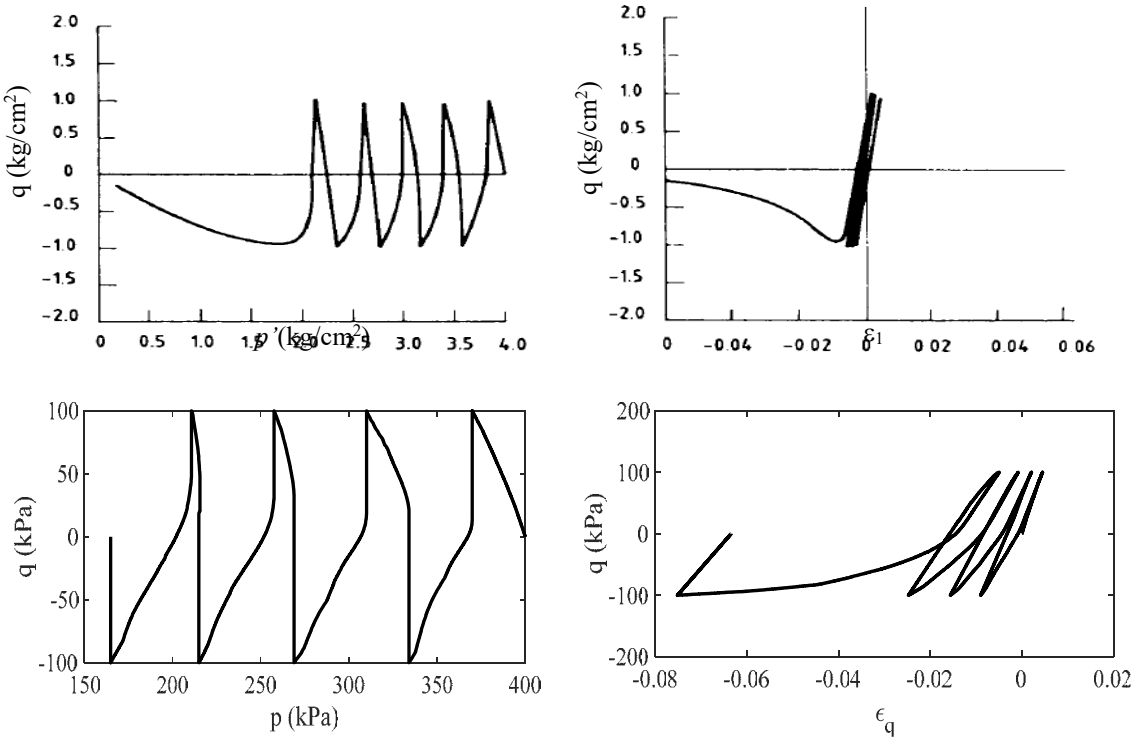

Figure 4: Simulation of two way stress-controlled undrained cyclic triaxial test, data of Pastor et al. (1985)

$$\sigma_{ij,j} + \rho g_i = \rho \ddot{u}_i \tag{27}$$

$$-p_{,i} + \rho_w g_i = \rho_w \ddot{u}_i + \frac{\dot{\bar{w}}_i}{k_i} \rho_w g_i \tag{28}$$

$$\dot{\varepsilon}_{ii} + \dot{\bar{w}}_{i,i} = -\frac{n}{K_f} \dot{p} \tag{29}$$

where for the material parameters; ρ is total density of soil, ρ_w is density of the water, n is porosity, K_f is bulk modulus of the pore water, g is the gravitational acceleration and k_i is the permeability coefficient. As for variable unknowns, $\sigma_{ij,j}$ is the divergence of total stress, u is solid part's displacement, $\bar{w}$ is the relative fluid displacement, p is the pore fluid pressure, $\ddot{u}_i$ is the acceleration of solid skeleton and $p_{,i}$ is the gradient of pore pressure, finally $\dot{\varepsilon}_{ii}$ is the rate of change of volumetric strain of the solid part.

3.2 Finite element formulation

Finite element (FE) formulation of the nonlinear dynamic analysis of coupled soil medium can be written using the Newton-Raphson iterative method and the Newmark time integration scheme. If we write the nonlinear equation of motion in matrix-vector form, we get:

$$\begin{bmatrix} \mathbf{M_s} & 0 \\ \mathbf{M_{sf}} & 0 \end{bmatrix} \begin{Bmatrix} \ddot{\boldsymbol{U}} \\ \ddot{\boldsymbol{P}} \end{Bmatrix}_{n+1} + \begin{bmatrix} 0 & 0 \\ \mathbf{C^T} & \mathbf{C_f} \end{bmatrix} \begin{Bmatrix} \dot{\boldsymbol{U}} \\ \dot{\boldsymbol{P}} \end{Bmatrix}_{n+1} + \begin{bmatrix} 0 & -\boldsymbol{C} \\ 0 & 0 \end{bmatrix} \begin{Bmatrix} \boldsymbol{U} \\ \boldsymbol{P} \end{Bmatrix}_{n+1} + \begin{Bmatrix} \boldsymbol{R}_s^{\text{int}} \\ \boldsymbol{R}_f^{\text{int}} \end{Bmatrix}_{n+1} = \begin{Bmatrix} \boldsymbol{R}_s^{ext} \\ \boldsymbol{R}_f^{ext} \end{Bmatrix}_{n+1} \tag{30}$$

where $\mathbf{M_s}$ and $\mathbf{M_{sf}}$ are the mass matrices of the solid phase and the coupled system, $\mathbf{C}$ is coupling matrix, $\mathbf{C_f}$ is the fluid compressibility matrix. $\boldsymbol{R}_s^{\text{int}}$ is the internal force of the solid part, and $\boldsymbol{R}_f^{\text{int}}$ is the internal force based on flow of fluid part, $\boldsymbol{R}_s^{ext}$ and $\boldsymbol{R}_f^{ext}$ are the external load vectors associated with the solid and the fluid part, hence water. The nonlinear equation of motion is written in general form as below:

$$\underset{\sim}{\tilde{M}}\ddot{\underset{\sim}{X}}_{n+1} + \underset{\sim}{\tilde{C}}\dot{\underset{\sim}{X}}_{n+1} + \underset{\sim}{\tilde{K}}\underset{\sim}{X}_{n+1} + \underset{\sim}{R}^{int}_{n+1} = \underset{\sim}{R}^{ext}_{n+1} \tag{31}$$

X is the vector involving both solid and fluid part's degree of freedoms namely, displacement, U and pore pressure, P. Nonlinear formulation of the coupled system yields:

$$\left[\frac{1}{\beta\Delta t^2}\underset{\sim}{\tilde{M}} + \frac{\gamma}{\beta\Delta t}\underset{\sim}{\tilde{C}} + \left(\underset{\sim}{\overset{\sim}{\hat{K}}}^{tan}\right)^i_{n+1}\right]\partial\underset{\sim}{X}^{i+1}_{n+1} = \begin{Bmatrix} \left(\underset{\sim}{R}^{ext}\right)_{n+1} - \left(\underset{\sim}{R}^{int}\right)^i_{n+1} - \left[\frac{1}{\beta\Delta t^2}\underset{\sim}{\tilde{M}} + \frac{\gamma}{\beta\Delta t}\underset{\sim}{\tilde{C}}\right]\left(\underset{\sim}{X}^i_{n+1} - \underset{\sim}{X}_n\right) \\ + \underset{\sim}{\tilde{M}}\left[\frac{1}{\beta\Delta t}\dot{\underset{\sim}{X}}_n + \left(\frac{1}{2\beta} - 1\right)\ddot{\underset{\sim}{X}}_n\right] + \underset{\sim}{\tilde{C}}\left[\left(\frac{\gamma}{\beta} - 1\right)\dot{\underset{\sim}{X}}_n + \Delta t\left(\frac{\gamma}{2\beta} - 1\right)\ddot{\underset{\sim}{X}}_n\right] \end{Bmatrix} \tag{32}$$

where $\underset{\sim}{\overset{\sim}{\hat{K}}}^{tan}$ is the tangent stiffness matrix including the phase stiffness matrices and $\boldsymbol{C}$. In (32), γ and β are the Newmark parameters, i is the iteration number and n is the load step. (32) is solved for $\partial\underset{\sim}{X}^{i+1}_{n+1}$ at N number of iterations used to update incremental values as;

$$\Delta\underset{\sim}{U}^N_{n+1} = \sum_{i=1}^{N} \partial\underset{\sim}{U}^i_{n+1} \tag{33}$$

A residual force is calculated to check for convergence against a specified tolerance;

$$\left(\underset{\sim}{R}^{res}\right)^{i+1}_{n+1} = \underset{\sim}{R}^{ext}_{n+1} - \left(R^{int}\right)^{i+1}_{n+1} - \underset{\sim}{\tilde{M}}\ddot{\underset{\sim}{U}}^{i+1}_{n+1} - \underset{\sim}{\tilde{C}}\dot{\underset{\sim}{U}}^{i+1}_{n+1} \le TOL \tag{34}$$

3.3 FE Results

In this section, dynamic response of a 10m high soil column is analysed under harmonic load through the updated UBCSAND model. A computational FE model is developed and nonlinear finite element analyses are performed on a saturated porous sand soil using the coupled flow and deformation theory. The model parameters are obtained from Pastor et al. (1985). Figure 5 shows the variation of displacement, pore pressure and effective stress in

time for various depths. Though the pore pressures seem to rise unboundedly, failure seem to occur due to liquefaction in a short amount of time.

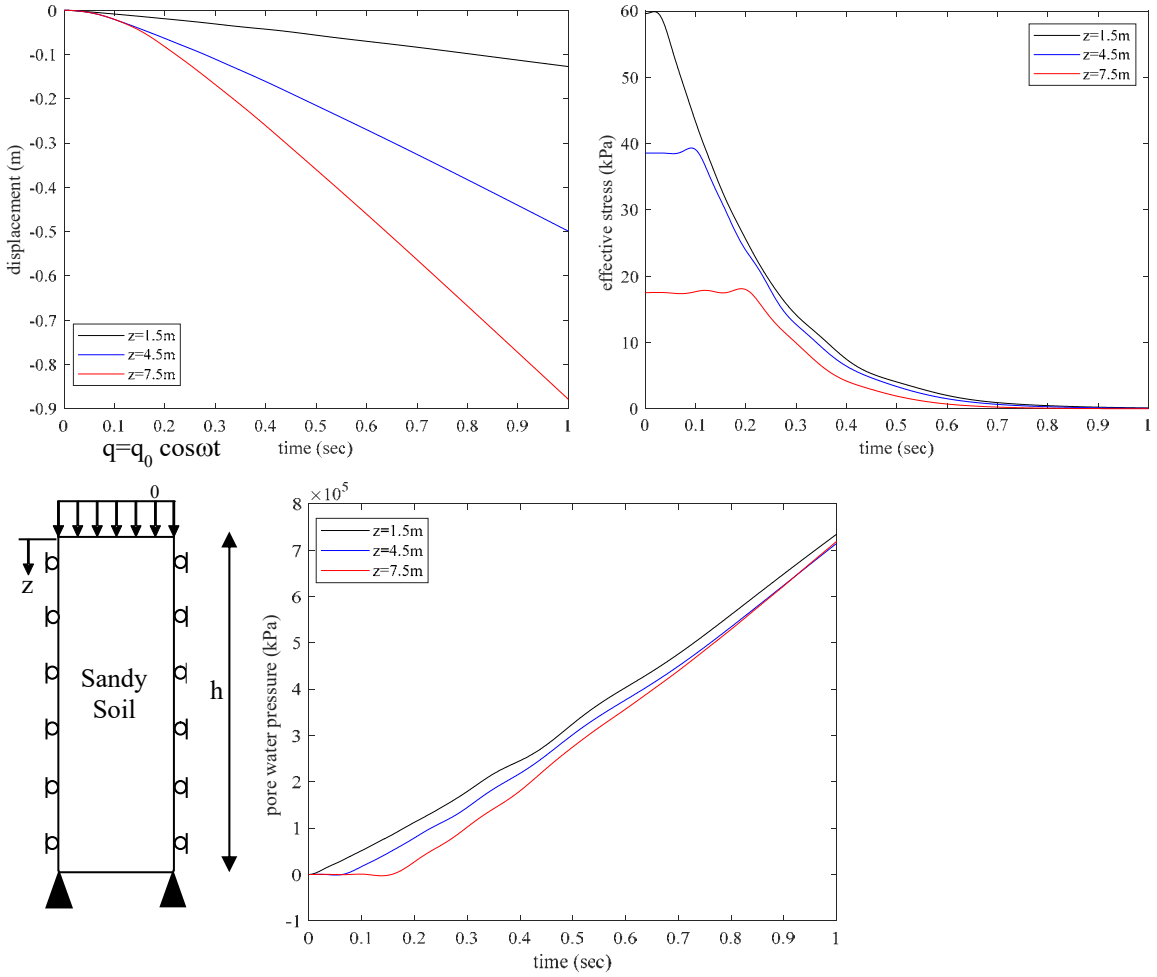

Figure 5: FE analysis results for a sandy soil column under surface harmonic excitation, T=0.1s, k=1e^{-4}m/s

4 CONCLUSIONS

In this study, cyclic response of loose sand is studied through elastoplastic analyses using the finite element method. First the UBCSAND constitutive model is evaluated generating results that are compared with available static and cyclic triaxial tests used to calibrate the model. Next, the calculation of plastic hardening modulus is updated using a proposed interpolation rule. The new rule accounts for the relative location of the current stress vector on the secondary surface acting as a yield surface in comparison to its value on the primary surface acting now as a bounding surface in the model. Then, the Generalized Plasticity Theory is adapted in the current formulation of the UBCSAND in terms of the deviatoric hardening rule using deviatoric plastic strains. Furthermore, the model is modified to serve with the generalized plasticity framework to evaluate the cyclic behavior of sands. Such an inclusion

of the theory led to better verification with corresponding undrained triaxial test results as opposed to its original formulation. Finally the latest update of the model is implemented into a newly developed 1-D finite element code and the harmonic response of a sandy soil column which is governed by the Biot's poroelasticity theory, is evaluated. A set of poro-elastoplastic analyses conducted indicate the effectiveness of the proposed interpolation rule along with the effect of the inclusion of basic definitions of the GPT which is found to be quite useful.

REFERENCES

[1] Pastor, M., Zienkiewicz, O. C., & Leung, K. H. Simple model for transient soil loading in earthquake analysis. II. Non-associative models for sands. *International Journal for Numerical and Analytical Methods in Geomechanics*. (1985) **9**(5): 477-498.

[2] Pastor, M., Zienkiewicz, O.C. and Chan, A.C. Theme/feature paper: Generalized plasticity and the modeling of soil behavior. *Int. J. Num. Anal. Mthds Geomech.* (1990) **14**: 151-190.

[3] Puebla, H., Byrne, P. M., & Phillips, R. Analysis of CANLEX liquefaction embankments: prototype and centrifuge models. *Canadian Geotechnical Journal*. (1997) **34**(5): 641-657.

[4] Beaty, M., & Byrne, P. M. An effective stress model for predicting liquefaction behaviour of sand. In ASCE *Geotechnical Earthquake Engineering and Soil Dynamics III*. (1998), 766-777.

[5] Petalas, A., Galavi, V., & Brinkgreve, R.B.J. Validation and verification of a practical constitutive model for predicting liquefaction in sands. In *Proceedings of the 22nd European young geotechnical engineers conference,* Gothenburg, Sweden, (2012), 167-172.

[6] Petalas, A. and Galavi, V. Plaxis Liquefaction Model UBC3DPLM. *PLAXIS Report*. (2013).

[7] Eliadorani, A. A. *The Response of Snads Under Partially Drained States With Emphasis on Liquefaction*, Doctoral Dissertation, University of British Columbia, Vancouver, Canada, (2000).

[8] Tatlıoğlu, E. Numerical Modeling of Poroelastic Seabed Soil –Structure Systems Under Cyclic Loading in Geotechnical Coastal Engineering (Doctoral Dissertation), Istanbul Technical University, Turkey (2018) (in Turkish).

[9] Tsegaye, A. B. Liquefaction Model UBC3D. PLAXIS Report. (2010).

[10] Ulker, M.B.C. 'Constitutive Modeling of Static Response of Clays Using Generalized Plasicity Theory', 16th National Conference on Soil Mechanics and Geotechnical Engineering, October 13-14, Atatürk University, Erzurum, Turkey, (2016) (in Turkish).

[11] Biot, M.A. General theory of three-dimensional consolidation. *J. Appl. Physics* (1941) **12**(2): 155-164.

[12] Biot, M.A. Theory of elasticity and consolidation for a porous anisotropic solid. *Journal of Applied Physics*. (1955) **26**(2): 182-185.

[13] Biot, M.A. Mechanics of deformation and acoustic propagation in porous media. *Journal of Applied Physics*. (1962) **33**(4): 1482-1498.